

# Hot Spots and Pseudogaps for Hole- and Electron-Doped High-Temperature Superconductors.

David Sénéchal<sup>1</sup> and A.-M.S. Tremblay<sup>1,2</sup>

<sup>1</sup>*Département de physique and Regroupement québécois sur les matériaux de pointe,*

<sup>2</sup>*Institut canadien de recherches avancées, Université de Sherbrooke, Sherbrooke, Québec, Canada, J1K 2R1*  
(Dated: August 2003)

Using cluster perturbation theory, it is shown that the spectral weight and pseudogap observed at the Fermi energy in recent Angle Resolved Photoemission Spectroscopy (ARPES) of both electron and hole-doped high-temperature superconductors find their natural explanation within the  $t$ - $t'$ - $t''$ - $U$  Hubbard model in two dimensions. The value of the interaction  $U$  needed to explain the experiments for electron-doped systems at optimal doping is in the weak to intermediate coupling regime where the  $t - J$  model is inappropriate. At strong coupling, short-range correlations suffice to create a pseudogap but at weak coupling long correlation lengths associated with the antiferromagnetic wave vector are necessary.

Deep insight into the nature of strongly correlated electron materials, such as high temperature superconductors, has emerged in the last few years from both experiment and theory. On the experimental side, ARPES [1] and scanning-tunneling experiments [2] provide us with detailed information on the nature of single-particle states. This information must be explained by theory if we are to understand correlated materials. For example, contrary to one of the central tenets of Fermi liquid theory, sharp zero-energy excitations are not enclosing a definite volume in the Brillouin zone. Certain directions are almost completely gapped while others are not. This is the famous pseudogap problem that has been the focus of much attention in the field [3].

On the theoretical side, Dynamical Mean-Field Theory (DMFT) [4] has allowed us to understand the evolution of single-particle states during the interaction-induced (Mott) transition between metallic and insulating states [5] (parent compounds of high-temperature superconductors are Mott insulators). Generalizations of DMFT, such as the Dynamical Cluster Approximation (DCA) [6] and Cellular-DMFT [7] are however necessary to take into account the momentum dependence of the self-energy that is neglected in DMFT and is clearly apparent in ARPES experiments [1]. Up to now, these calculations have been restricted to hole-doped systems and small system sizes or to the perfectly nested case. The nature of single-particle excitations, and in particular the pseudogap in cuprate superconductors, is thus still an open theoretical problem.

Without any assumption about the nature of the ground state, we show that the Hubbard model with fixed first-, second- and third-neighbor hopping ( $t$ ,  $t'$  and  $t''$ ) accounts for the strikingly different locations of low energy excitations observed experimentally in hole- and electron-doped cuprate superconductors [8, 9]. At zero doping we have a Mott insulator with a large  $U$ . By contrast with previous attempts to obtain a unified model [10], we will see that the interaction strength  $U$  varies as one moves from the hole-doped to the electron-

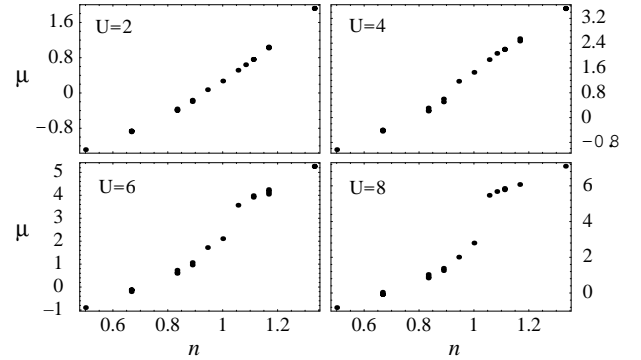


FIG. 1: Chemical potential calculated at various dopings using CPT, in units of  $t$ , the NN hopping. For this figure only,  $t' = -0.4t$  and  $t'' = 0$ .

doped systems. That parameter should be at least of the order of the bandwidth for hole-doped systems. In this case the pseudogap is controlled mainly by Mott Physics with short-range correlations. The situation is similar for underdoping with electrons. As we approach the optimally-doped electron case, the pseudogap occurs at a smaller coupling where Mott Physics is not essential. Long correlation lengths then play an essential role in creating the pseudogap whereas in the strong coupling case they are not necessary for the pseudogap to appear. These results give insight into two different mechanisms for the pseudogap phenomenon and into the nature of the breakdown of Fermi-liquid theory in these systems. We also gain insight into the appropriate microscopic model of high-temperature superconductors.

*Model and methodology.* We study the square lattice Hubbard model with on-site Coulomb repulsion  $U$ . We set the first-neighbor hopping  $t$  to unity, and introduce second-neighbor (diagonal) hopping  $t' = -0.3t$  and third-neighbor hopping  $t'' = 0.2t$ , as suggested by band structure calculations [11]. The diagonal hopping  $t'$  is a key ingredient to understand the Physics, even though its precise value can vary slightly between different compounds.

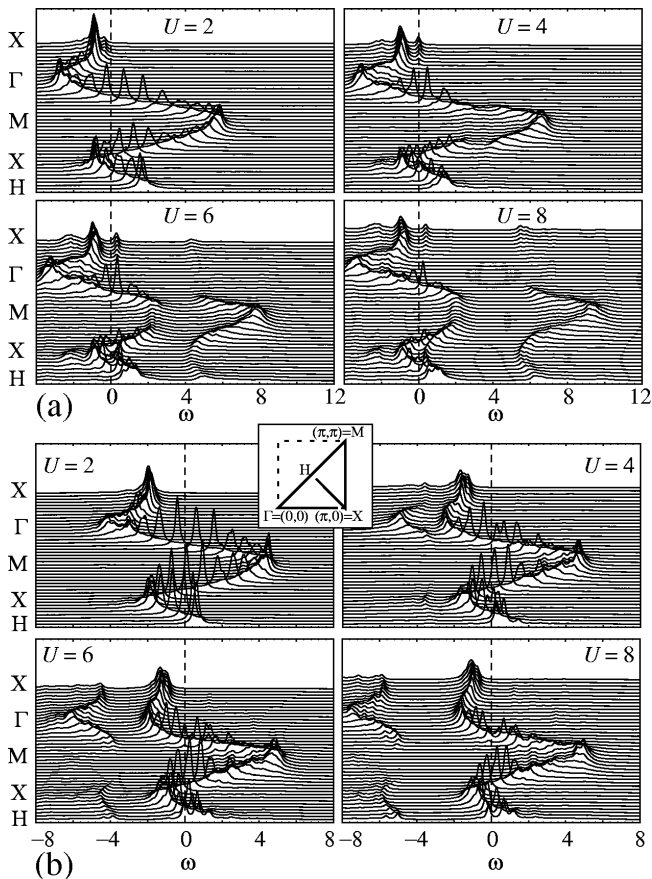


FIG. 2: Single particle spectral weight, as a function of energy  $\omega$  in units of  $t$ , for wavevectors along the high-symmetry directions shown in the inset. (a): CPT calculations on a  $3 \times 4$  cluster with 10 electrons (17% hole doped). (b): the same, with 14 electrons (17% electron doped). In all cases we use  $t' = -0.3t$  and  $t'' = 0.2t$ . A Lorentzian broadening  $\eta = 0.12t$  is used to reveal the otherwise delta peaks.

It frustrates antiferromagnetic (AFM) order and removes particle-hole symmetry, thereby also allowing the AFM zone boundary to cross the Fermi surface. The third-neighbor hopping  $t''$  makes the Fermi surface slightly bulge away from the intersection with the AFM zone boundary, as observed experimentally [8], and makes low-energy excitations more stable along the diagonal of the Brillouin zone.

We use Cluster Perturbation Theory [12] (CPT) to gain insight into the single-particle states of the Hubbard model and their relation to cuprate superconductors. The method can reproduce the spin-charge separation of one dimensional systems [12] as well as the dispersion relations obtained in the large  $U$  limit. It reduces to the exact result at  $U = 0$  and in the atomic limit ( $t_{ij} = 0$ ). It is based on exact diagonalizations of finite clusters that are coupled through strong-coupling perturbation theory. It basically amounts to replacing the exact self-energy by that of the cluster only [13]. The Green function calculated by CPT is made up of a set

of discrete poles, like in ordinary exact diagonalizations, except that (i) more poles have substantial weight and (ii) they disperse continuously with wavevector, allowing for clear momentum distribution curves. The results presented here were calculated on 12-site rectangular clusters. The resulting Green function is averaged over the  $(3 \times 4)$  and  $(4 \times 3)$  clusters to recover the original symmetry of the lattice. We checked that the main features are the same when using clusters of different shapes. Our finite energy resolution, of about  $0.12t$ , does not allow us to resolve effects related to superconductivity. We compare with ARPES experiments of similar resolution.

*The Mott transition.* We begin in Fig. 1 with a plot of the chemical potential  $\mu$  as a function of doping for various values of the interaction strength. The different results in this figure are obtained from clusters of different sizes ranging from 4 to 13 sites with varying geometry. The smooth behavior of the function away from half-filling shows that the cluster sizes are large enough to provide reliable results. There is a jump in  $\mu$  when  $U$  is large enough, namely above  $U = 6t$  roughly. The jump in  $\mu$  does not follow from a long-range ordered ground state since the basic clusters are finite. It is instead a clear manifestation of the Mott phenomenon.

Fig. 2 displays the single-particle spectral weight  $A(\mathbf{k}, \omega)$  as a function of energy for wave vectors  $\mathbf{k}$  along the high-symmetry directions shown in the inset. Only the  $\omega < 0$  domain of  $A(\mathbf{k}, \omega)$  is accessible to ARPES. Fig. 2(a) illustrates the effect of increasing interaction strength on a near optimally hole-doped system while Fig. 2(b) does the same in the electron-doped case. Clearly, there is a range of frequencies where  $A(\mathbf{k}, \omega) = 0$  for *all* wave vectors. This is the Mott gap. At finite doping it always opens up away from zero energy when  $U$  is sufficiently large. In the electron-doped case,  $\omega = 0$  is in the upper Hubbard band. The lower Hubbard band is at negative energies, as has been observed in ARPES [14]. The overall narrowing of the band just below the Fermi level is more important in the electron-doped case. Also, the shape of the dispersion is different from that obtained in a mean-field AFM state [15] and there is no clear doubling of the dispersion relation of the type that occurs in one dimension when there is spin-charge separation.

*Fermi surface plots and pseudogap.* We now move to the main point of our paper, namely the pseudogap and hot spots. The top two panels of Fig. 3 for a 17% hole-doped system represent the strength of  $A(\mathbf{k}, \omega)$  at  $\omega = 0$ . As a function of interaction strength, the intensity disappears gradually near the  $(\pi, 0)$  and  $(0, \pi)$  points, leaving zero-energy excitations only near the diagonal. Large values of  $U$  ( $U > 8t$ ) seem necessary to reproduce the experimentally observed spectral function of hole-doped systems [9], even more so on a 11% doped system (not shown). The lower panels show the imaginary part of the self-energy (or scattering rate) corresponding to the momentum-dispersion curve right above. For  $U = 2t$ ,

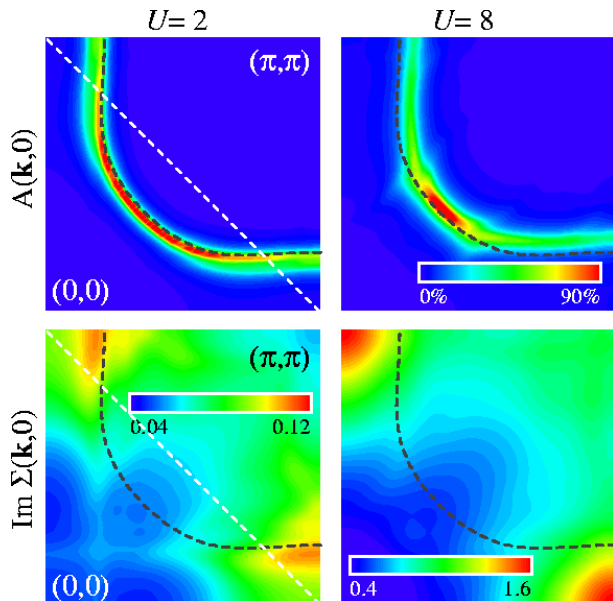


FIG. 3: (color) Top: Intensity plot of the spectral function at the Fermi level, in the first quadrant of the Brillouin zone, for a 17% hole-doped system (10 electrons on a  $3 \times 4$  cluster). Here  $t' = -0.3t$  and  $t'' = 0.2t$  (the gray dashed line is the non-interacting Fermi surface). Bottom: Imaginary part of the self-energy (in units of  $t$ ) corresponding to the same parameters as the top plot. A Lorentzian broadening is used:  $\eta = 0.12t$  (top) and  $\eta = 0.4t$  (bottom).

the self-energy is very small overall, but has a maximum along the Fermi surface where the Fermi velocity is smallest (density of states largest); this illustrates how we depart from the Fermi liquid picture (in which  $\Sigma''(0) = 0$ ) as we move towards intermediate coupling. At  $U = 8t$ , the scattering rate is much larger and affects larger regions separated by roughly  $(\pi, \pi)$ . In all cases a higher scattering rate leads to removal of spectral weight.

The electron-doped case is displayed in Fig. 4 for 17% doping. At moderate  $U$ , the spectral intensity drops only at the intersection of the AFM Brillouin zone with the Fermi surface. However, for larger  $U$ , only the neighborhoods of  $(\pi, 0)$  and  $(0, \pi)$  survive. The latter situation is analogous to that observed by ARPES in electron underdoped systems and can be reproduced by calculations (not shown) with  $U$  large at 11% doping. At optimal doping however, ARPES results [14] look instead qualitatively like the upper left panel of Fig. 4.

*Hot spots and pseudogap.* The Fermi-surface points where the intensity decreases (Fig. 4) are called hot spots. However, a pseudogap is characterized not only by lower intensity at the Fermi energy, but also by a dispersive peak that stops short of crossing the Fermi surface. This experimentally well-known phenomenon is illustrated on Fig. 5, which shows energy dispersion curves for wave vectors along the  $(\pi, 0) - (\pi, \pi/2)$  stretch in the hole-doped case (left) and along the diagonal in the electron-doped case (right). For small values of  $U$ , a well-defined quasi-

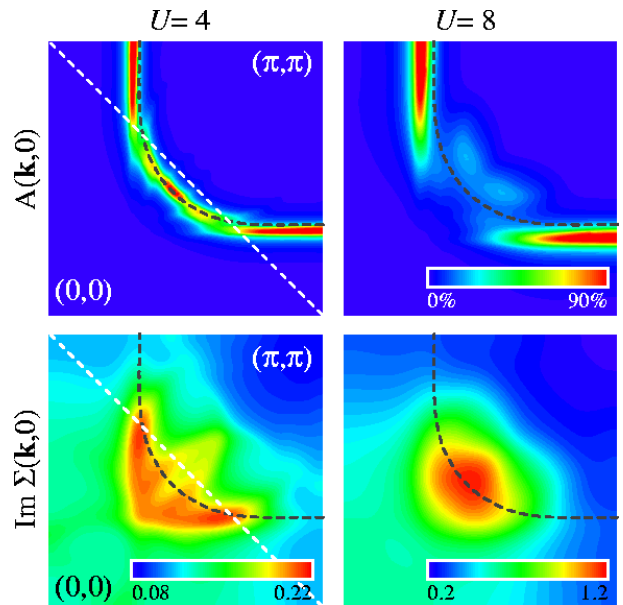


FIG. 4: (color) Same as Fig. 3, but for an electron-doped system (14 electrons on a  $3 \times 4$  cluster). The white dashed line on the left panels is the AFM zone boundary, showing the coincidence of hot spots with the intersection of this line with the Fermi surface.

particle exists at the Fermi level ( $\omega = 0$ ). At stronger coupling ( $U = 8t$ ), a pseudogap comparable to experimental observation is clearly visible at the Fermi level.

*Discussion: strong- and weak-coupling pseudogaps.* As in previous studies, the strong-coupling pseudogap [16] is concomitant with the Mott gap but is clearly distinct from the latter. The Mott gap is a purely local (on-site) phenomenon that occurs for all wave vectors and is not tied to  $\omega = 0$ . By contrast, the pseudogap occurs around  $\omega = 0$  and only in regions of the Fermi surface that are connected to other such regions by wave vectors that have a broad spread of radius  $\delta$  around  $(\pi, \pi)$ . The difference in the location of the pseudogap between hole- and electron underdoped cuprates follows by simply finding which points of the Fermi surface can be connected by  $(\pi, \pi)$ , within  $\delta$ , to other Fermi surface points.

Despite the importance of  $(\pi, \pi)$ , the strong-coupling pseudogap is not caused by long-range AFM correlations. Indeed, (a) Our lattices do not exhibit long-range order (b) We verified that the results are not very sensitive to  $t'$  (frustration) (c) Fig. 5 shows that at  $U > 8t$  the pseudogap is of order  $t$ , only weakly dependent on  $U$  and does not scale as the antiferromagnetic coupling  $J = 4t^2/U$ , in contrast with previous studies [16, 17]. This pseudogap would therefore persist in the  $U \rightarrow \infty$  limit of the Hubbard model, where hopping between sites is constrained by the impossibility of double occupancy and where  $t$  is the relevant energy scale. For a case where it is possible to study the size dependence of the strong-coupling pseudogap at fixed doping, we verified that the

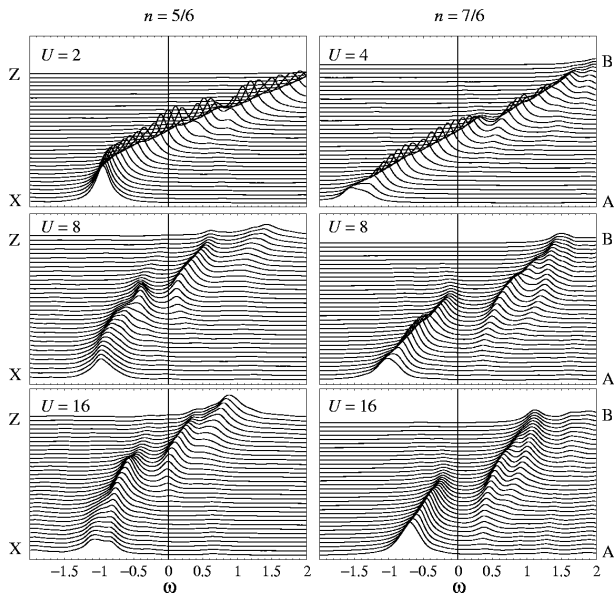


FIG. 5: Left: Spectral function for the hole doped system illustrated in Figs. 2a and 3 plotted as a function of energy, for wavevectors along the direction  $X = (\pi, 0)$  to  $Z = (\pi, \pi/2)$ . At  $U = 2t$  (top), a depression in the spectral function is visible slightly away from  $\omega = 0$ , while the pseudogap is fully opened at  $U = 8t$  (middle). Right: Spectral function for the electron-doped system illustrated in Figs 2b and 4, plotted along the diagonal of the Brillouin zone, from  $A = (0.3\pi, 0.3\pi)$  to  $B = (0.7\pi, 0.7\pi)$ . The results for the experimentally relevant electron underdoped system are similar.

results are size independent, suggesting again the short-range nature of the phenomenon. Longer range correlations at the AFM wave vector might only reinforce the strong-coupling pseudogap that already exists in the presence of short-range correlations. The location of this strong-coupling pseudogap, in both electron- and hole-doped cases, coincides with the predictions of the umklapp mechanism [18], which does not need long-range correlations. However, a proper strong-coupling extension of the umklapp mechanism is still needed.

Signs of a pseudogap also occur at weak coupling. This is illustrated by the hot spots that are visible in the electron-doped case at  $U = 4t$  in Fig. 4, upper panel. Contrary to the  $U = 8t$  case, these hot spots (a) are located precisely at the intersection with the AFM zone boundary (b) they generally correspond to a cluster shape dependent depression in  $A(\mathbf{k}, \omega)$  and not to a genuine pseudogap. We attribute these results to the short correlation lengths (limited to the cluster size) in CPT and conclude that we are seeing the onset of the true pseudogap that, as expected from the presence of true gaps in the itinerant antiferromagnet [19], would be induced by large AFM correlation lengths [20]. We find, as in Ref. [20], that the interaction strength  $U$  cannot be larger than  $U \approx 6t$  to preserve this kind of pseudogap where  $\omega = 0$  excitations persist near the diagonal.

Since experiments on optimally-doped electron superconductors do find large AFM correlation lengths [21] as well as  $\omega = 0$  single-particle excitations [8] near the diagonal, the pseudogap mechanism in this case should be the weak-coupling one ( $U \lesssim 6t$ ) [19, 20]. This value of  $U$  is smaller than, but not too different from, that necessary for a sizeable Mott gap at half-filling. This may be understood as follows. The contribution to the value of  $U$  that comes from simple Thomas-Fermi screening scales like  $(\partial\mu/\partial n)$ . Fig. 1 clearly shows that this quantity, beginning at  $U > 4t$ , is smaller for electron-doped than for hole-doped systems, demonstrating the internal consistency of a picture where the value of  $U$  decreases as one goes from the hole- to the electron-doped systems. Ref. [20] presents additional arguments for a smaller  $U$ .

To summarize, we illustrated two ways in which a Fermi liquid can be destroyed by a pseudogap and found that a unified picture of  $A(\mathbf{k}, \omega)$  in the cuprates emerges from the  $t - t' - t'' - U$  model if we allow  $U$  to decrease as the concentration of electrons increases.

We are indebted to B. Kyung, V. Hankevych, K. Le Hur and J. Hopkinson for useful discussions. The present work was supported by the Natural Sciences and Engineering Research Council (NSERC) of Canada, the Fonds québécois de la recherche sur la nature et les technologies (FQRNT), the Canadian Foundation for Innovation, and the Tier I Canada Research Chair Program (A.-M.S.T.).

- 
- [1] A. Damascelli *et al.*, Rev. Mod. Phys. **75**, 473 (2003).
  - [2] J. Hoffmann *et al.*, Science **297**, 1148 (2002).
  - [3] T. Timusk and B. Statt, Rep. Prog. Phys. **62**, 61 (1999).
  - [4] A. Georges *et al.*, Rev. Mod. Phys. **68**, 13 (1996).
  - [5] M. Imada *et al.*, Rev. Mod. Phys. **70**, 1039 (1998).
  - [6] T.A. Maier *et al.*, Phys. Rev. B **66**, 075102 (2002).
  - [7] C. J. Bolech *et al.*, Phys. Rev. B **67**, 75110 (2003).
  - [8] N. Armitage *et al.*, Phys. Rev. Lett. **86**, 1126 (2001).
  - [9] F. Ronning *et al.*, Phys. Rev. B **67**, 165101 (2003).
  - [10] C. Kim *et al.*, Phys. Rev. Lett. **80**, 4245 (1998).
  - [11] O. Andersen *et al.*, J. Phys. and Chem. Solids **56**, 1573 (1995).
  - [12] D. Sénéchal *et al.*, Phys. Rev. Lett. **84**, 522 (2000); D. Sénéchal *et al.*, Phys. Rev. B **66**, 075129 (2002).
  - [13] C. Gros *et al.*, Phys. Rev. B **48**, 418 (1993).
  - [14] N. Armitage *et al.*, Phys. Rev. Lett. **88**, 257001 (2002).
  - [15] C. Kuskó *et al.*, Phys. Rev. B **66**, 140513 (2002).
  - [16] T. D. Stanescu *et al.*, Phys. Rev. Lett. **91**, 017002 (2003).
  - [17] K. Haule *et al.*, Phys. Rev. Lett. **89**, 236402 (2002).
  - [18] N Furukawa *et al.*, J. Phys.: Condens. Matter **10**, L381 (1998); C. Honerkamp *et al.*, Phys. Rev. B **63**, 035109 (2001).
  - [19] R.S. Markiewicz cond-mat/0308469; H. Kusunose *et al.* Phys. Rev. Lett. **91**, 186407 (2003).
  - [20] B. Kyung *et al.*, Phys. Rev. B **68**, 174502 (2003); cond-mat/0312499; Y.M. Vilk *et al.*, J. Phys. I France **7**, 1309 (1997).
  - [21] P. Mang *et al.*, cond-mat/0307093. H.J. Kang *et al.*, Nature **423**, 522 (2003).